Fluorescent Single-Stranded DNA Binding Protein as a Probe for Sensitive, Real-Time Assays of Helicase Activity

Mark S. Dillingham,* Katherine L. Tibbles,† Jackie L. Hunter,† Jason C. Bell,‡§ Stephen C. Kowalczykowski,‡§ and Martin R. Webb†

*DNA:Protein Interactions Unit, Department of Biochemistry, School of Medical Sciences, University of Bristol, Bristol, United Kingdom; †MRC National Institute for Medical Research, London, United Kingdom; ‡Section of Microbiology, Center for Genetics and Development, University of California at Davis, Davis, California; and §Section of Molecular and Cellular Biology, Center for Genetics and Development, University of California at Davis, Davis, California

ABSTRACT The formation and maintenance of single-stranded DNA (ssDNA) are essential parts of many processes involving DNA. For example, strand separation of double-stranded DNA (dsDNA) is catalyzed by helicases, and this exposure of the bases on the DNA allows further processing, such as replication, recombination, or repair. Assays of helicase activity and probes for their mechanism are essential for understanding related biological processes. Here we describe the development and use of a fluorescent probe to measure ssDNA formation specifically and in real time, with high sensitivity and time resolution. The reagentless biosensor is based on the ssDNA binding protein (SSB) from *Escherichia coli*, labeled at a specific site with a coumarin fluorophore. Its use in the study of DNA manipulations involving ssDNA intermediates is demonstrated in assays for DNA unwinding, catalyzed by DNA helicases.

INTRODUCTION

Single-stranded DNA (ssDNA) is a key intermediate in most cellular DNA transactions, including replication, transcription, repair, and recombination. Therefore, the separation of double-stranded DNA (dsDNA) into two lengths of ssDNA is an important part of many such processes. DNA helicases promote this unfavorable reaction by coupling it to ATP hydrolysis, and unwind DNA with rates typically between 10 and 1000 basepairs (bp) per second (1).

Our understanding of such DNA processing, and its regulation, requires appropriate assays for helicase activity so that it can be followed in real time. A fluorescent reporter has the potential to provide the required combination of high sensitivity and time resolution. Several fluorescence-based assays have been developed to monitor helicase activity at both the bulk and single-molecule level by probing the physical separation of oligonucleotide strands (2–4). These assays generally have a label on each strand, such as a FRET pair. When done on the adjacent 5′ and 3′ ends, such labeling gives a signal at the end of the oligonucleotide separation, and these ''all or none'' assays have the advantage of providing high resolution over short distances. In bulk assays with long dsDNA, the signal change becomes unsynchronized and resolution is lost. Only a few types of assays are suitable for continuously monitoring the processive unwinding of long stretches (kilobases) of dsDNA, and these generally require measuring the disappearance of dsDNA or the appearance of ssDNA (5,6). There are several DNA-binding dyes that provide fluorescence signals to monitor transformation of dsDNA to ssDNA (6,7). Many bind specifically in the grooves of dsDNA and the fluorescence decreases on release from the DNA as strand separation occurs. However, this type of probe may not be suitable for low extents of reaction because it measures the concentration of substrate and thus relies on measuring a small decrease of fluorescence against a large background. Moreover, dsDNA-binding dyes have the potential to inhibit the reaction being studied. Reagentless biosensors based on fluorescent proteins have been used successfully in a number of cases to provide rapid probes of concentrations of molecules formed in biological assays (8–10), such as phosphate (11), glucose (12), and maltose (13). Such biosensors are single molecular species that interact with the molecule of interest, giving a fluorescence change that can be used to monitor the change in concentration. The fluorescence can be extrinsic, via a label attached to the protein, or intrinsic (for example, using an intrinsically fluorescent protein fused with the binding protein).

The requirements for a biosensor include specificity for the target molecule, in particular with discrimination against similar molecules that may also be present in the assay mixture. In the case described here, an assay must discriminate between ssDNA and a large excess of dsDNA. The ssDNA binding protein (SSB) from *Escherichia coli* has potential for use in such a biosensor. Several prokaryotic SSB proteins have been investigated and there are high-resolution structures of SSB from *E. coli* with and without DNA (14,15). SSB exists as a tetramer that can bind ~70 bases of DNA at high salt concentrations (16), and the crystal structure shows DNA wrapped around a tetramer. Particularly at low salt, SSB can bind a ~35 base length of ssDNA. The protein binds DNA rapidly and tightly, but the mechanism may be complex due to DNA wrapping around the tetramer

Submitted March 14, 2008, and accepted for publication June 10, 2008.

Address reprint requests to Dr. Martin R. Webb, Tel.: 44-20-8816-2078; Fax: 44-20-8906-4477; E-mail: mwebb@nimr.mrc.ac.uk.

Editor: Taekjip Ha.

0006-3495/08/10/3330/10 $2.00

doi: 10.1529/biophysj.108.133512

(17). Binding is apparently cooperative and there may be interaction between neighboring SSB tetramers along a strand of ssDNA. A decrease in tryptophan fluorescence, when SSB binds to DNA, has been used as a probe for DNA strand separation (5) and SSB-DNA interactions (18). Recently, the phage T4 gp32 protein, also a ssDNA-binding protein but structurally distinct from SSB, was modified with a fluorescein derivative to provide a probe for ssDNA in a study of the T4 recombination system (19). Here, we report the modification of *E. coli* SSB with an extrinsic fluorophore to provide a sensitive probe for ssDNA. This probe outperforms alternative methods for detecting processive helicase activity based on fluorescent binding dyes or intrinsic tryptophan fluorescence.

MATERIALS AND METHODS

Materials

AddAB (AddA^{D1172A}B^{D961A} mutant) and RecBCD were purified as described previously (20,21). The PcrA and RepD proteins and the pCERoriD plasmid were generous gifts from Dr. P. Soultanas (University of Nottingham) and Dr. C. Thomas (University of Leeds). Linearized pCERoriD substrates were prepared by digestion with either the HinDIII, AvaII, or *Eco*RI restriction endonuclease (New England Biolabs, Ipswich, MA) to generate substrates with the oriD initiation site positioned at different distances from the DNA ends (22). The pBR322 and pADF0 plasmids were purified using Maxiprep kits (Qiagen, Valencia, CA) and cesium chloride density gradient centrifugation, and then linearized with the *Eco*RI or ClaI restriction endonucleases. The restriction enzymes were heat-inactivated. Agarose gel analysis confirmed efficient linearization, and the plasmid substrates were not purified further. ssRNA, as a ladder of seven lengths, and Lambda DNA were obtained from New England Biolabs, and poly(U) and poly(dT) were obtained from Sigma-Aldrich (Gillingham, UK). The concentrations of these nucleic acids are given in terms of nucleotides. dT_{35} and dT_{70} were obtained from Eurogentec, and concentrations are given in terms of moles of oligonucleotide.

The coumarin labeling reagents, IDCC (*N*-[2-(iodoacetamido)ethyl]-7-diethylaminocoumarin-3-carboxamide) and MDCC (*N*-[2-(1-maleimidyl) ethyl]-7-diethylaminocoumarin-3-carboxamide), and the single isomer rhodamine iodoacetamide, 6-IATR (6-iodoacetamidotetramethylrhodamine), were synthesized and provided by Dr. J. E. T. Corrie (NIMR, London, UK) (23,24). Other fluorescent labeling reagents were obtained from Invitrogen (Carlsbad, CA).

Mutant SSB proteins

The wild-type *E. coli* ssb gene was cloned into a pET15b vector (Novagen, Nottingham, UK) using PCR with primers containing flanking NdeI and BamHI restriction sites. This vector was used as a template for site-directed mutagenesis using the QuikChange kit (Stratagene, La Jolla, CA) to produce genes for G26C or S92C SSB. The pET15b constructs were sequenced (DBS sequencing facility, UC Davis) to confirm the presence of the desired mutations and the integrity of the remainder of the ssb gene. The mutated genes were then transferred to pET22b vectors using the NdeI and BamHI restriction sites, and these were used to transform *E. coli* (BL21-DE3 pLysS, Novagen) for overexpression using the T7 promoter system. Cells were grown in 2 L of LB at 37°C to mid-log phase and expression was induced with 1 mM IPTG. After 3 h the cells were harvested, resuspended in 50 mL of 50 mM Tris·HCl pH 7.5, 200 mM NaCl, 1 mM EDTA, 1 mM dithiothreitol, and 10% sucrose, and stored at –80°C.

The mutant SSB proteins were purified at 4°C using a modification of the method of Lohman et al. (25). The cell suspension was thawed and 0.1 mM PMSF was added. Cell lysis by sonication was followed by centrifugation. The supernatant was collected and polymin P (10% stock solution, pH 6.9) was added slowly to 0.4%, followed by constant stirring for 15 min. A pellet was collected by centrifugation at 10K for 20 min and then completely resuspended in 50 mL of 50 mM Tris·HCl pH 8.3, 20% glycerol, 1 mM EDTA, and 0.4 M NaCl using a Dounce homogenizer, followed by stirring for 30 min. Insoluble material was removed by centrifugation at 10K for 20 min. Solid ammonium sulfate was added very slowly to the supernatant to give 150 g l^{-1}. After stirring for 30 min, the pellet was collected by centrifugation at 13K for 30 min. The pellet was resuspended in 50 mL of 50 mM Tris·HCl pH 8.3, 20% glycerol, 1 mM EDTA, and 0.2 M NaCl. The resuspension was centrifuged at 18K for 20 min and passed through a 0.2-μm syringe filter. A 5-mL Hi-Trap heparin column (GE Healthcare, Little Chalfont, UK) was equilibrated in 50 mM Tris·HCl pH 8.3, 20% glycerol (v/v), 1 mM EDTA. The sample was loaded at a low salt concentration by mixing with equilibration buffer (in the ratio 16:84 for sample/buffer volume) immediately before the column in the mixing chamber of the chromatography apparatus. This is necessary because SSB is prone to precipitation if kept for extended periods at the low salt concentration required for binding to heparin. The column was then washed with equilibration buffer and SSB was eluted with a 150-mL gradient from 0 to 1 M NaCl in this buffer. Peak fractions were pooled, dialyzed extensively against storage buffer (20 mM Tris·HCl pH 8.3, 1 mM EDTA, 0.5 M NaCl, 50% glycerol (v/v), and 1 mM dithiothreitol (DTT)), and stored at –80°C. Protein concentration was determined by measuring absorbance at 280 nm using a theoretical extinction coefficient of 111,520 $M^{-1}cm^{-1}$ for the tetramer. A mass spectrum gave a mass of 18,893 $\pm$ 3 Da; the theoretical mass is 18,890 Da, assuming cleavage of the N-terminal methionine. The protein is >95% pure as judged by SDS-PAGE analysis.

Modification of mutant SSB proteins with fluorescent dyes

Cysteine mutants of SSB were covalently modified with a variety of fluorescent dyes. The protocol below was used to label G26C SSB with the diethylaminocoumarin iodoacetamide (IDCC). The other dyes and mutant SSB adducts were prepared similarly, but with some variation in length of time or concentrations of reactants.

An aliquot of SSB (G26C) (5 mg in 1.3 mL) was incubated with DTT for 10 min in 20 mM Tris·HCl pH 7.5, 1 mM EDTA, 500 mM NaCl, 20% glycerol. The DTT was removed from the protein using a PD10 column (GE Healthcare), pre-equilibrated in the same buffer that had been degassed by bubbling nitrogen. IDCC, in twofold excess over monomers, was added to the ~25 μM protein tetramer and incubated under nitrogen for 2 h at room temperature with end-over-end stirring and protection from light. Excess IDCC was removed by reaction with sodium 2-mercaptoethane sulfate (10-fold excess over protein monomers) for 10 min. The incubation mixture was filtered through a membrane (0.2 μm pores, polyethersulfone from Whatman, Maidstone, UK). The protein was isolated by passing through a P4 gel filtration column (BioRad; 1 × 30 cm), pre-equilibrated in 20 mM Tris·HCl pH 8.3, 1 mM EDTA, 500 mM NaCl, 20% glycerol. The protein concentration was calculated from the coumarin absorbance at 430 nm, where the extinction coefficient is 44800 $M^{-1}cm^{-1}$, assuming it is the same as IDCC (23). Glycerol was added to the labeled protein (DCC-SSB) to 50% (v/v), which was then stored at −80°C. A mass spectrum gave a mass of 19,237 $\pm$ 3 Da; the theoretical mass is 19,233 Da. Concentrations given for DCC-SSB are for the tetramer, unless otherwise stated.

Absorbance and fluorescence measurements

Absorbance spectra were obtained on a Beckman (Fullerton, CA) DU640 spectrophotometer in 25 mM Tris·HCl pH 7.5, 200 mM NaCl, 1 mM DTT. Fluorescence measurements were generally obtained at high ionic strength, 25 mM Tris·HCl pH 7.5, 200 mM NaCl, 1 mM DTT, and 5 μM bovine serum albumin, on a Cary Eclipse fluorimeter (Varian, Palo Alto, CA) with a xenon lamp, using 3-mm-pathlength cells. For low ionic strength conditions, the NaCl concentration was reduced to 20 mM. Quantum yields were measured

at 20°C in 1-cm-pathlength cells using solutions with absorbance of ~0.03 cm^{-1} at the exciting wavelength. The corrected emission spectra were obtained from 435 to 600 nm. The quantum yields were measured relative to Coumarin 343, which has a known value of 0.63 (26).

Stopped-flow experiments were carried out on a HiTech SF61MX apparatus (TgK Scientific Limited, Bradford-on-Avon, UK), with a mercury-xenon lamp and HiTech IS-2 software. There was a monochromator and 4-mm slits on the excitation light, and an appropriate cutoff filter on the emission (436 nm excitation and 455 nm filter for DCC-SSB, 366 nm excitation and 400 nm filter for dye displacement). In all stopped-flow measurements described here, the stated concentrations are those in the mixing chamber, unless shown otherwise. Data were fitted to theoretical curves using either the HiTech software or Grafit 5 (27).

Specificity tests

Lambda DNA was heat-denatured by heating the following solution for 5 min at 95°C: 261 μM DNA (in terms of nucleotides), 50 mM Tris·HCl pH 7.5, 10% (v/v) sucrose, 2 mM magnesium acetate, 2 mM dithiothreitol. The product was put on ice and used immediately. ssRNA was heat-denatured and used in the same way.

Titration data fitting

For the titrations of DNA into a solution of SSB, where there was likely to be more than one mode of binding, data were fitted to the appropriate competition equilibria, as described below. Because the titrations were at relatively high concentration of SSB, it is assumed that there was tight binding and so essentially no free DNA until in excess over SSB. This assumption made it possible to derive equations for the observed fluorescence, depending on the fluorescence of each DCC-SSB complex, when the concentration of DNA was less than that of SSB. Above this concentration, the fluorescence remains constant at its maximum.

dT_{70} was titrated into a solution containing equimolar fluorescent SSB and unlabeled SSB:

$$\Delta Fluorescence = (F_{max} - F_{min})(-b + \mathrm{sqrt}(b^2 + 4(K-1)PL))/(2L(K-1))). \quad (1)$$

Where $b = KX + P + L - KP$, X = [unlabeled SSB], L = [DCC-SSB], P = [total dT_{70}], K = ratio of K_d values for the two SSB species, F_{min} = fluorescence in the absence of DNA, F_{max} = fluorescence of DCC-SSB·dT_{70}.

dT_{70} was also titrated into a solution of DCC-SSB at low salt, where ''35 base'' binding is significant. In this mode, it is assumed the predominant species is dT_{70}·2DCC-SSB at low DNA. As more DNA is added, the main species becomes dT_{70}·SSB. There is a competition between these two species depending on the ratio, K nM, of the two dissociation constants (that for complete dissociation of dT_{70}·2DCC-SSB/dT_{70}·DCC-SSB). At any point in the titration with DNA<DCC-SSB, [dT_{70}·2DCC-SSB] is given by:

$$D_{S2} = (K + L - \mathrm{sqrt}((K+L)^2 - 4(LP - P^2)))/2. \quad (2)$$

So that:

$$Observed\,fluorescence = (F_3(P - D_{S2}) + F_2 D_{S2} + (L - P - D_{S2}))/L, \quad (3)$$

where L = [DCC-SSB], P = [total dT_{70}], F_3 is the fluorescence of dT_{70}·DCC-SSB, and F_2 is that of dT_{70}·2DCC-SSB, relative to that of DCC-SSB.

dT_{35} was also titrated into a solution of DCC-SSB at low salt. In this case, ''35 base'' binding gives dT_{35}·DCC-SSB, but as more DNA is added it is assumed that $2dT_{35}$−DCC-SSB forms. Thus there are two consecutive equilibria as one and then two dT_{35} molecules bind. The proportion of each complex depends on the ratio of these two dissociation constants, K (that for dissociation of one dT_{35} from each of dT_{35}·DCC-SSB/$2dT_{35}$·DCC-SSB). At any point in the titration with dT_{35}<2DCC-SSB, [dT_{35}·DCC-SSB] is given by:

$$D_S = (-L + \mathrm{sqrt}(L^2 - (4K-1)(P^2 - 2LP)))/(4K-1). \quad (4)$$

So that:

$$Observed\,fluorescence = (0.5F_3(P - D_S) + F_2 D_S + F_1(L - 0.5P - 0.5D_S))/L, \quad (5)$$

where L = [DCC-SSB], P = [total dT_{35}], F_3 is the fluorescence of $2dT_{35}$·DCC-SSB, and F_2 is the fluorescence of dT_{35}·DCC-SSB, relative to that of DCC-SSB.

Helicase assays

All experiments were performed at 37°C. All data presented are representative single trace measurements with no averaging. For measurements of PcrA helicase activity, experiments were performed by preincubating 25 nM PcrA and 4 nM RepD (monomer) with 1 nM pCERoriD DNA substrate (6.2 μM nucleotides) in a buffer containing 50 mM Tris·HCl pH 7.5, 10 mM $MgCl_2$, 100 mM KCl, and 1.1 μM DCC-SSB (monomer) for 5 min. The reaction was initiated by rapid mixing with an equal volume of 0.5 mM ATP in the same buffer. The protocol for this experiment is essentially identical to that performed previously (22), except that the wild-type *Bacillus subtilis* SSB has been directly replaced with DCC-SSB. For measurements of RecBCD helicase-nuclease activity, experiments were performed by preincubating 5 nM (saturating) RecBCD with 1 nM ClaI-linearized pADGF0 DNA (6.1 μM nucleotides) in a buffer containing 25 mM Tris-acetate pH 7.5, 2 mM magnesium acetate, 1 mM DTT, and 1.1 μM DCC-SSB (monomer) for 5 min. The reaction was initiated by rapid mixing with 1 mM ATP in the same buffer. The fluorescence signals were calibrated using heat-denatured Lambda DNA under identical solution conditions and instrument settings. For the measurements of AddAB activity, experiments were performed by preincubating 2.5 nM $AddA^{D1172A}B^{D961A}$ with 0.1 nM (870 nM nucleotides) *Eco*RI-linearized pBR322 DNA (unless stated otherwise), in a buffer containing 25 mM Tris·HCl pH 7.5, 2 mM $MgCl_2$, 175 nM DCC-SSB (monomer), and either 20 mM (low ionic strength) or 200 mM (high ionic strength) NaCl for 5 min. The reaction was initiated by rapid mixing with an equal volume of 0.5 mM ATP in the same buffer. For the dye displacement assay, the DCC-SSB was replaced with wild-type SSB and the buffer was supplemented with 200 nM Hoechst 33258 dye. The fluorescence signals were calibrated using heat-denatured *Eco*RI-linearized pBR322 under identical solution conditions (both high and low salt) and instrument settings. Calibration with heat-denatured Lambda DNA produced virtually identical results. For all experiments, the unwinding data are plotted in arbitrary fluorescence units and as apparent nanomolar ssDNA (in nucleotides), based on the calibrations. It should be noted that the measurement is of SSB binding, rather than of ssDNA per se, and that these values may differ if ssDNA is produced in a form that cannot be bound by the SSB protein (for example, if there is extensive nuclease activity).

RESULTS

Wild-type SSB from *E. coli* contains no cysteines. Therefore, the first stage of investigating the potential of SSB as the basis of a biosensor was to choose positions for introduction of a single cysteine as the site to attach a fluorescent label. The crystal structures suggest that there are only minor changes in protein subunit conformation on association with DNA (14,15). In wrapping around the surface of the tetramer, DNA winds through a series of channels in the protein sur-

face. Single cysteines were introduced into the protein on loops that are at the top of such channels. One mutation (S92C) is in a loop that is essentially unaltered between the two structures. Another mutation (G26C) is on a loop that may be flexible in the DNA-free structure, but is well defined in the DNA-bound form. In either case, wrapping DNA around the SSB surface provides a significant opportunity for changes in the fluorophore environment. Therefore, we chose to survey several fluorophores that are sensitive to environmental factors to determine which label might be best suited for this work (Table 1). For this survey, conditions for labeling and for isolation of the labeled protein were not optimized. The fluorescence change was assessed mainly using a model ssDNA substrate, dT_{70}, that is very likely to bind only one tetramer under the conditions used, but also to fill the binding channel of a tetramer completely (16).

Major optical criteria for assessing a molecule suitable for solution measurements include the size of the fluorescence increase on binding DNA, as well as having a reasonably high fluorescence quantum yield. Out of the labels tested, the two diethylaminocoumarins gave the largest fluorescence change. SSB G26C, labeled with the coumarin IDCC (DCC-SSB), was chosen for further study for two reasons. First, it consistently gave the largest fluorescence increase. Second, it does not have the potential complications of forming a chiral center on reaction with a thiol. For example, in the case of MDCC, reaction of its maleimide with a cysteine within a protein gives two diastereoisomers that may have different fluorescence properties (11). In contrast, it is likely that reaction of IDCC with a thiol produces a single molecular species. The final labeling and purification conditions for DCC-SSB are described in the Materials and Methods section.

Fluorescence properties of DCC-SSB

Fig. 1 shows the change in fluorescence spectra when DCC-SSB binds dT_{70}. The fluorescence enhancement of ~6-fold was similar when poly-dT was used. The fluorescence quantum yield of DCC-SSB was measured to assess fluorescence of the probe in absolute terms, as described previously (11). The quantum yield is 0.03 in the absence of DNA and 0.15 in the presence of saturating dT_{70}, and there is essentially no change in absorbance of the coumarin on binding DNA. Note that the quantum yield reflects the area of the emission peak, rather than intensity at a particular wavelength. In comparison, the diethylaminocoumarin, attached to a small molecule in aqueous medium, has a low quantum yield (<0.05) (11,28). This suggests that in the absence of DNA, the fluorescence of the coumarin in DCC-SSB is largely unaffected by the attached protein. Presumably, the coumarin is not interacting significantly with the protein surface.

A titration of dT_{70} into a solution of DCC-SSB at high ionic strength produces an almost linear increase in fluorescence, followed by a sharp break as the maximum fluorescence is maintained (Fig. 1 *b*). The linear increase is consistent with tight binding of DNA to SSB, and the break point is at the expected stoichiometry of one SSB tetramer per dT_{70} molecule.

To determine the effect of labeling on the affinity of SSB for ssDNA, dT_{70} was titrated into a mixture of unlabeled SSB and DCC-SSB (Fig. 1 *b*). The resulting curve was analyzed in terms of the two proteins having different affinities. This analysis gives the ratio of the dissociation constants with the unlabeled protein binding as 28-fold tighter. However, the labeled protein still binds DNA very tightly, even in the high salt conditions used in this study: a titration of dT_{70} into 2.5 nM DCC-SSB tetramers (Fig. 2) gave an estimate of ~2.6 nM for the apparent K_d value. The smaller percent fluorescence change in this titration is due to light scattering becoming relatively significant at this low concentration and thus adding significantly to the background. Fig. 2 *b* shows that the fluorescence increases linearly with concentration for both DNA-free and DNA-bound DCC-SSB.

Nucleic acid specificity

The specificity of the response was measured for other nucleic acid species (Table 2). Lambda dsDNA gave no re-

TABLE 1 Fluorescence changes for a survey of various mutant SSB: dye combinations

			Fluorescence ratio ($\pm$ dT_{70})	
Fluorescent label	Extinction wavelength (nm)	Emission wavelength (nm)	S92C	G26C
IDCC*	430	477	2.8	6.1
MDCC*	430	477	2.2	4.9
MIANS*	436	474	0.4	–
6-IATR*	553	576	1.3	2.8
Alexa Fluor 488 maleimide	495	518	3.1	3.3
Alexa Fluor 546 maleimide	560	574	1.5	2.3
Fluoroscein-5-maleimide	493	520	–	3.8

Fluorescence spectra of 250 nM labeled SSB (tetramer concentration) were measured at 30°C in 25 mM Tris·HCl pH 7.5, 200 mM NaCl, 1 mM DTT, and 5 μM bovine serum albumin. Excitation was at the appropriate wavelength for the fluorophore, and the emission intensities at the maximum were measured in the absence and presence of saturating dT_{70}.

*IDCC is *N*-[2-(iodoacetamido)ethyl]-7-diethylaminocoumarin-3-carboxamide); MDCC is *N*-[2-(1-maleimidyl)ethyl]-7-diethylaminocoumarin-3-carboxamide; MIANS is 2-(4′-maleimidylanilino)naphthalene-6-sulfonic acid; 6-IATR is 5-iodoacetamidotetramethylrhodamine.

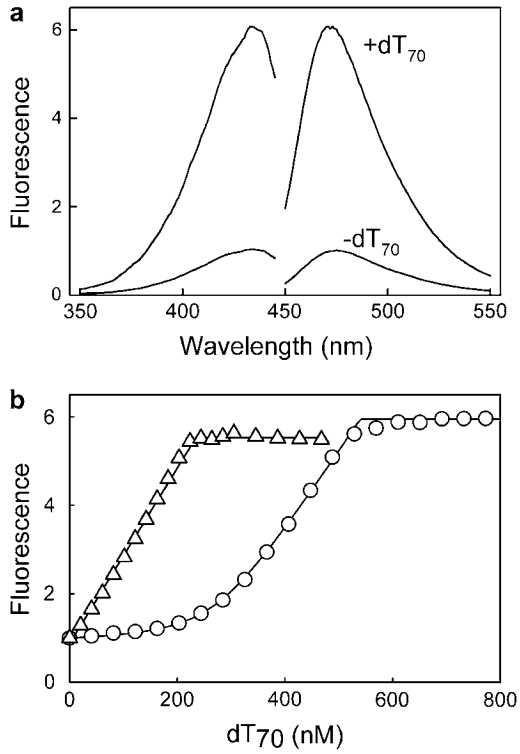

FIGURE 1 Fluorescence spectra and titration of DCC-SSB with dT_{70}. Measurement conditions were as in Table 1. (*a*) Excitation and emission spectra of 100 nM DCC-SSB, in the presence and absence of 580 nM dT_{70}. Excitation was at 433 nm, emission at 476 nm. (*b*) Titration of emission intensity (excitation at 430 nm, emission 475 nm) as a function of dT_{70} added to 250 nM DCC-SSB tetramer (*triangles*) in 60 μL. The lines are the best linear fit up to 233 nM dT_{70}, and the best fit horizontal line for remaining points. In the competition titration, aliquots of dT_{70} were added to a mixture of unlabeled SSB (S92C) and DCC-SSB (*circles*). The concentrations were nominally 220 nM of each protein tetramer. The ordinate is the extent of formation of DCC-SSB·dT_{70}, as measured by the fluorescence. It is apparent that low concentrations of DNA bind mainly to the unlabeled SSB, as there is only a small increase in fluorescence in this region. This implies that the unlabeled protein has the higher affinity. The data were fitted as described in Materials and Methods. The line shows the best fit for which the ratio of K_d(DCC-SSB)/K_d(SSB) is 28. To show that this change in affinity is not specific to the coumarin label, the measurement was done with 6-IATR-labeled G26C SSB and gave a similar result (data not shown).

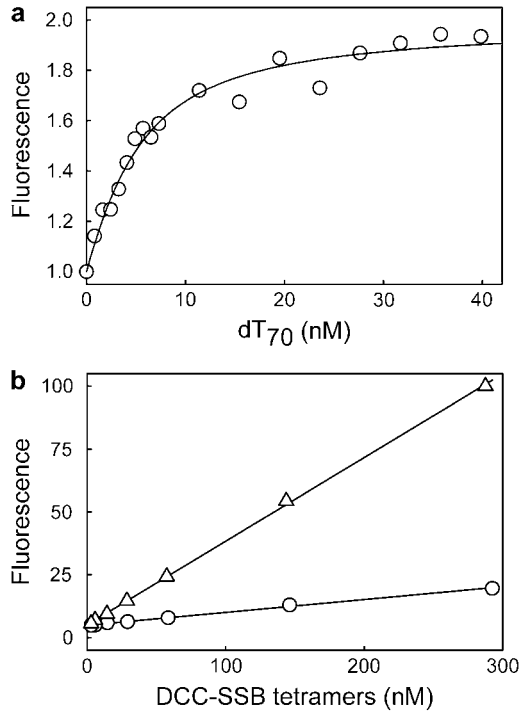

FIGURE 2 Response of DCC-SSB at low concentrations. Fluorescence measurements and solution conditions were the same as in Fig. 1b. (*a*) Titration of dT_{70} into a solution of 2.5 nM DCC-SSB tetramers in 80 μL. The data were fitted to a quadratic equation for equilibrium binding of a ligand to a fluorescent protein, as described previously (38). This fit gives a value of K_d as 2.6 nM. (*b*) Change in fluorescence with concentration of DCC-SSB in the presence (*triangles*) and absence (*circles*) of DNA. The concentration of dT_{70} was 500 nM. At low concentrations the background scatter becomes significant, but the fluorescence intensities and fluorescent change all have a linear dependence over the whole concentration range.

sponse, but after heat treatment to separate the strands, it gave approximately the full fluorescence increase. ssRNA (before or after heat treatment) also gave no response. The presence of 175 μM poly(U) (concentration in terms of nucleotides) had essentially no effect on a titration of dT_{70} into 125 nM DCC-SSB tetramers. These data suggest that DCC-SSB is highly selective for ssDNA, as previously reported for wild-type protein (16).

Effect of ionic strength

All the measurements described above were at high ionic strength (200 mM NaCl). At low salt concentrations, the binding mode of SSB to DNA may differ from that at high salt (16): under some circumstances, ~35-base lengths of DNA are the preferred ligands for SSB. In addition, binding affinities and fluorescence properties may be affected by ionic strength. To get a basic picture of the effect of ionic strength on the fluorescence properties of DCC-SSB as it interacts with DNA, a series of titrations were performed (Fig. 3). dT_{70} and dT_{35} were used as the DNA ligands at low (20 mM NaCl) and high ionic strength (200 mM NaCl), titrating into a fixed amount of DCC-SSB. The DCC-SSB concentration employed was relatively high (284 nM), so the binding was likely to be stoichiometric as the concentration of DNA increased.

The titration of dT_{70} at high salt, shown in Fig. 3 *a*, is equivalent to that in Fig. 1 *b*: there is an approximately linear increase in fluorescence until the SSB is saturated at ~1 dT_{70}/SSB. In contrast, at low ionic strength there is a break in the titration at approximately half saturation. This is consistent with the SSB tetramer binding ~35-base length of DNA at low dT_{70} concentrations, until each dT_{70} has two tetramers bound (dT_{70}·2SSB). This binding mode gives a smaller fluorescence increment, even accounting for the fact that only half the monomers are likely to be interacting with DNA. It may mean that in this binding mode, only one coumarin per tetra-

TABLE 2 Summary of fluorescence increases with various nucleic acids

Nucleic acid	Fluorescence ratio
dT_{70}	5.3
dT_{70}*	4.8
dT_{35}†	5.1
dT_{35}*†	3.8
Poly(dT)	4.7
Lambda DNA (heat-denatured)	4.3
Lambda DNA (native)	1.0
ssRNA (heat-denatured)	1.0
Poly(U)	1.1

Measurements typically used 100 nM DCC-SSB in 60 μl 25 mM Tris·HCl pH 7.5, 200 mM NaCl, 1 mM DTT, and 5 μM bovine serum albumin, with conditions as in Fig. 1. A twofold excess of the nucleic acid was added, except as shown, calculated on the basis of a 70-base binding site. The fluorescence increase is given at 470 nm as a ratio of (+ nucleic acid)/(− nucleic acid).

*Low salt conditions: the buffer contained 20 mM NaCl.

†A fourfold molar excess of dT_{35} was used.

mer may be influenced significantly by DNA binding. At higher dT_{70} concentrations, there is a steeper increase in fluorescence. Either another dT_{70} adds to the dT_{70}·2SSB complex or, more likely, there is a rearrangement to a one-to-one dT_{70}−SSB complex, similar to that at high ionic strength. The data were fitted to a model in which the two binding modes compete as described in Materials and Methods and Fig. 3.

The titrations with dT_{35} have been plotted with the abscissa scale half that of the dT_{70} titrations. In this way, the scales are equivalent considering the total length of DNA added and, therefore, the degree of saturation of the SSB binding sites. The dT_{35} titrations are unaffected by salt at low DNA concentrations, but diverge at high concentrations. At high ionic strength, there is a break at ~1 dT_{35}/SSB-tetramer, after a linear rise in fluorescence. The steeper rise in fluorescence as more DNA is added is similar to the dT_{70} low salt curve. Following the model above, dT_{35}·SSB is formed first. Then the steeper increase in fluorescence would be due to formation of a $2dT_{35}$·SSB-tetramer complex; that is, the two short DNA lengths together fill the whole of the tetramer binding site. These data were fitted to a model with these two complexes competing as described in Materials and Methods and Fig. 3. At low salt, the similar rise in the fluorescence at low added DNA suggests a similar formation of a one-to-one dT_{35}·SSB-tetramer complex. Overall, the titration is fairly linear. It is possible that the addition of a second dT_{35} is governed by a weaker affinity and/or a smaller fluorescence increment. Some implications of this model and the effects of ionic strength on the use of DCC-SSB in helicase assays are discussed further below.

Association kinetics

To assess the applicability of DCC-SSB as a probe for kinetic assays, it is important to know the feasible rates of DNA

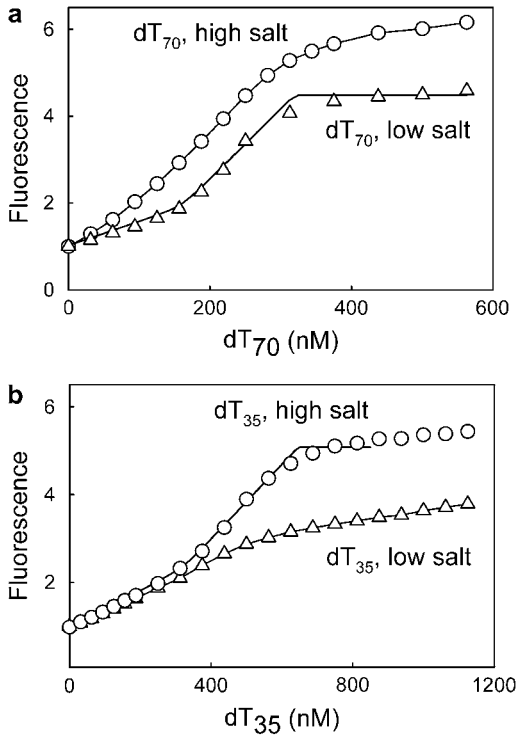

FIGURE 3 Effect of ionic strength on fluorescence signals. Titrations were performed as in Fig. 1. Low ionic strength conditions had 20 mM NaCl. The solutions contained 284 nM DCC-SSB tetramers. The data for dT_{70} at low ionic strength and dT35 at high strength were fitted as described in Materials and Methods. For the low-salt dT_{35} data, the line shows the best fit, for which the ratio of fluorescence intensities for DCC-SSB:dT_{35}·DCC-SSB:$2dT_{35}$·DCC-SSB is 1:2.3:5 and the ratio of dissociation constants of one dT_{35} from each complex (dT_{35}·DCC-SSB/$2dT_{35}$·DCC-SSB) is 0.002. For the low-salt dT_{70} data, the line shows the best fit for which the ratio of fluorescence intensities for DCC-SSB:dT_{70}·2DCC-SSB:dT_{70}·DCC-SSB is 1:1.8:4.4 (per SSB) and the ratio of dissociation constants for complete dissociation (dT_{70}·2DCC-SSB/dT_{70}·DCC-SSB) is 1.6 nM. However, in neither case is the dissociation constant ratio accurately determined by the fit. The other two lines are joining individual data points: the approximately linear rise in fluorescence precluded useful fitting to those models.

binding. Association kinetics, measured under pseudo first-order conditions with a large excess of dT_{70} over DCC-SSB (Fig. 4), gave a linear relation between rate constant and concentration over the range used. This slope is ~10^9 $M^{-1}s^{-1}$, suggesting that binding may be controlled by diffusion. Other work on the kinetics with wild-type protein has proposed a multistep pathway (16,17), and this is discussed further below.

Helicase assays

The DCC-SSB reagentless biosensor was used to monitor DNA unwinding catalyzed by DNA helicases. In the experiments presented below, DCC-SSB was employed at concentrations well above the measured K_d and at a stoichiometry of ~1 DCC-SSB monomer per 5 nucleotides substrate DNA, which ensures a linear fluorescence response

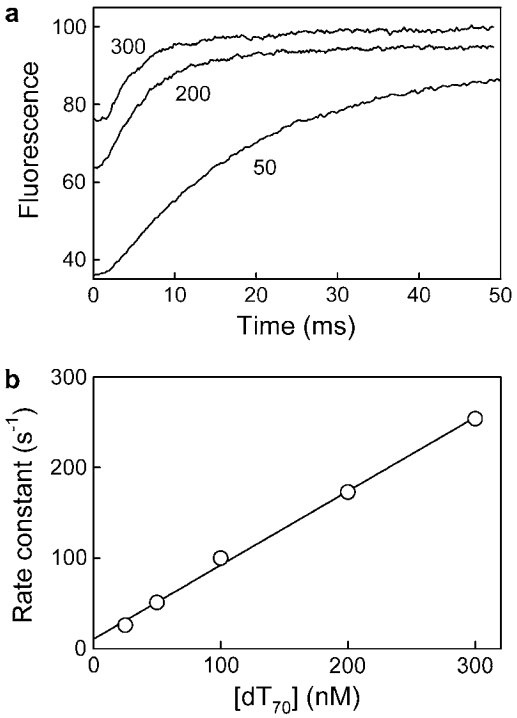

FIGURE 4 Association kinetics of DCC-SSB with dT_{70}. (*a*) A 5-nM DCC-SSB tetramer was mixed with various concentrations of dT_{70} and fluorescence intensity followed with time in a stopped-flow apparatus. Conditions were as in Table 1, except that measurements were performed at 25°C. Typical individual traces at nanomolar concentrations of dT_{70} are shown. Traces were normalized to finish at 100% and offset by 5% from each other. The fast traces have diminished amplitude, mainly due to loss of signal during the dead time of the instrument (~2 ms). Individual fluorescence traces fitted single exponentials well and the rate increased with DNA concentration. (*b*) Dependence of rate on concentration of DNA. Data shown are the averages of typically three traces from each of two separate experiments.

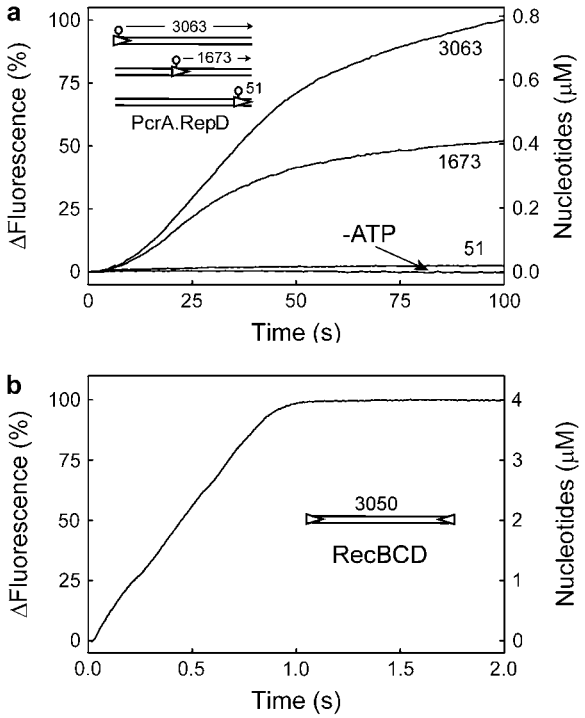

FIGURE 5 Use of DCC-SSB to monitor helicase activity of PcrA and RecBCD. Experimental details are given in Materials and Methods and the changes in fluorescence are in arbitrary units. (*a*) Unwinding of the three different lengths of DNA substrates, catalyzed by PcrA/RepD, monitored using DCC-SSB fluorescence. The schematic shows the linearized plasmid DNA: RepD initiator protein loads PcrA at oriD sites, and the helicase processively unwinds the duplex to the right of oriD. The distance (in basepairs) between the oriD and the end of the DNA is indicated. The ''-ATP'' control was on the longest DNA. (*b*) Linearized pADGF0 unwinding by saturating RecBCD, monitored using DCC-SSB fluorescence. The schematic shows the pADGF0 plasmid with the length of the DNA indicated. The sharp breakpoint in the trace suggests an unwinding rate of ~1700 bp s^{-1} per RecBCD.

regardless of SSB binding mode (see below for discussion). In one example (Fig. 5 *a*), three different lengths of dsDNA substrates are unwound by PcrA helicase, after nicking by RepD at the oriD origin (29,30). In each case, the dsDNA has the oriD site at a different position relative to one end. Unwinding by PcrA starting from oriD is unidirectional, and so each substrate is unwound to different extents by the helicase. The rates and extent of reactions are in good agreement with those determined under identical conditions using tryptophan fluorescence (22). However, the data are of much higher quality: averaging of multiple traces and significant corrections for photobleaching are avoided when extrinsic DCC fluorescence is used. Moreover, the use of DCC-SSB will allow facile analysis of the effect of PcrA and RepD concentrations on the observed unwinding, which has previously been limited by the background fluorescence from these components.

In a second example, we monitored DNA unwinding by the RecBCD helicase-nuclease, which is the fastest and most processive helicase reported in the literature (5,6,31). RecBCD is involved in the recombinational repair of DNA breaks and initiates unwinding from DNA ends. After the addition of ATP to preformed RecBCD·DNA complexes, there is a rapid linear fluorescence increase followed by a sharp breakpoint that marks the end of the unwinding reaction after ~0.9 s. This suggests an unwinding rate of ~1700 bp s^{-1} per RecBCD binding site (Fig. 5), in excellent agreement with previous estimates (32).

Finally, we investigated the unwinding of linearized plasmid DNA by a nuclease-deficient mutant of the *B. subtilis* AddAB helicase-nuclease (Fig. 6). AddAB is a functional analog of RecBCD that is also involved in the processing of DNA breaks for recombinational repair. It binds tightly to free DNA ends and, in the presence of ATP, translocates and unwinds DNA rapidly and processively (33). We directly compared the data from the DCC-SSB sensor with those from dye-displacement assays (6) at both low and high ionic strengths. At low ionic strength, AddAB unwinds >90% of the DNA substrate at a maximum observed rate of 400 nM ntds s^{-1} (equivalent to ~1000 bp s^{-1} per AddAB binding site). As would be expected for a DNA-

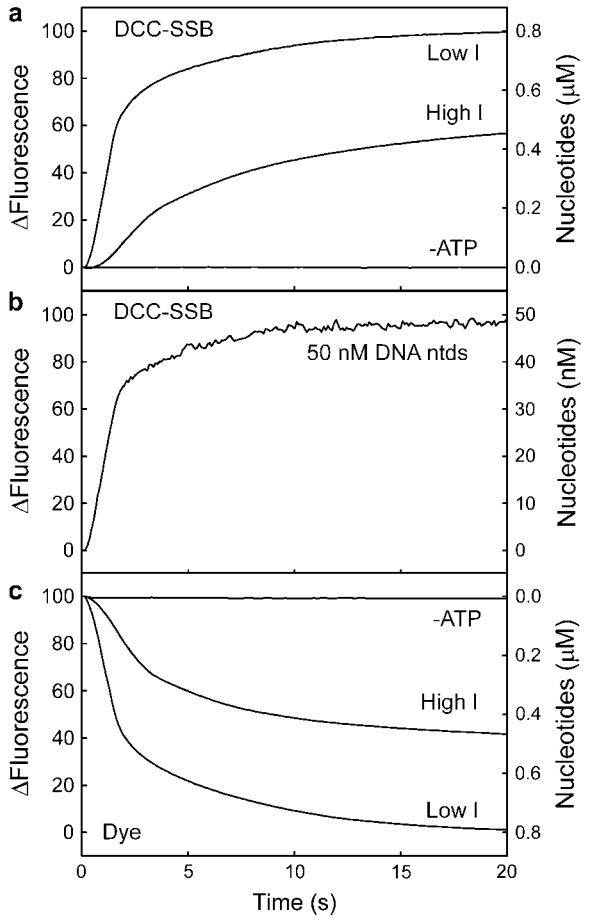

FIGURE 6 Comparison of DCC-SSB and dye displacement assays for the helicase AddAB. Experiments were performed as described in Materials and Methods. (*a*) DCC-SSB assay, at high and low ionic strengths and 37°C. The control shown is at low ionic strength in the absence of ATP. (*b*) DCC-SSB assay as in *a*, but with 50 nM (in nucleotides) pBR322. (*c*) Dye displacement assay. Experimental conditions were the same as in *a*, but the DCC-SSB was replaced with wild-type SSB and the buffer was supplemented with 200 nM Hoechst 33258 dye. The fluorescence signals were calibrated using heat-denatured *Eco*RI-linearized pBR322 under identical solution conditions (both high and low salt) and instrument settings.

binding protein, AddAB-catalyzed DNA unwinding is less effective at high ionic strength, and both the extent and the maximum observed rate (85 nM ntds s^{-1}) of the reaction are diminished. Importantly, however, the dye displacement assay produces traces similar to those obtained using DCC-SSB regardless of the ionic strength: the maximum observed rates are 340 and 110 nM ntds s^{-1}, respectively. As expected, the observed unwinding amplitude was proportional to the DNA substrate concentration, and a single trace measurement for 50 nM (in nucleotides) substrate DNA retained an excellent signal/noise ratio (Fig. 6 *b*).

DISCUSSION

DCC-SSB has a number of properties that make it suitable for solution assays of dsDNA unwinding. Optically, there is a large (sixfold) fluorescence increase on binding to ssDNA and a reasonably large Stokes shift, and so the requirements for light source and emission filtering are flexible. The excitation at 420–430 nm is not likely to affect other components in the assay mixture. In practice, for techniques such as stopped-flow, the Hg line at 436 nm provides a good light source. The labeled SSB exhibits tight binding under likely assay conditions, as described in the Results section. DCC-SSB is also highly selective for ssDNA over dsDNA or RNA, under the conditions used.

An important factor for kinetic assays is that the kinetics of DCC-SSB binding to ssDNA does not limit the observed rate. At 25°C, the binding is extremely rapid and may be diffusion-controlled at 10^9 $M^{-1}s^{-1}$. Indeed, the assays shown in Fig. 5 demonstrate the capability of DCC-SSB to measure helicase rates in excess of 1000 bp s^{-1}. A previous study of SSB association kinetics proposed multistep binding, with the first step likely to be diffusion-controlled, and estimated the dissociation rate constant as 0.044 s^{-1} at 25°C and 200 mM NaCl (34). A study at microsecond resolution using relaxation techniques identified a further step after the bimolecular binding process, and the results were interpreted in terms of the wrapping of DNA around the tetramer (17).

The fluorescence changes observed at high and low ionic strengths can be accommodated by the model in which there are two modes of DNA binding, as previously described (16). At low ionic strength and low ratio of DNA to SSB, ''35 base'' binding predominates and gives a smaller fluorescence change with DCC-SSB. In this mode, presumably the binding is predominantly on two of the four protein subunits. In other conditions, the ''70 base'' binding predominates: the DNA presumably binds all four monomers in the SSB tetramer and DCC-SSB gives a larger fluorescence change. The data fitting in Fig. 3 suggests that the fluorescence increase for free DCC-SSB to that bound in the ''35 base'' mode is not much more than a quarter of that to the ''70 base'' mode. Assuming that the fluorescence of all four coumarins is affected by dT_{70} (or $2dT_{35}$) binding in the ''70 base'' mode, then maybe only one coumarin is mainly affected in the ''35 base'' mode and another less so. The smaller fluorescence increment on ''35 base'' binding provides an explanation for the slight curvature in the titration with dT_{70} at high ionic strength (Fig. 1 *b*). Even at high ionic strength there may be a small proportion of this binding mode at a low DNA/SSB ratio.

The use of DCC-SSB avoids limitations of internal tryptophan fluorescence relating to a lack of sensitivity, photobleaching, and interference from other species, such as proteins and nucleic acids that absorb in the same UV range as tryptophan. In practice, we find that DCC-SSB is between one and two orders of magnitude more sensitive than using internal tryptophan fluorescence in equivalent helicase assays, where the maximal decrease in fluorescence is to one-third of the starting value, as opposed to an ~6-fold increase with DCC-SSB. Indeed, it is easily possible to detect the

unwinding of low nanomolar concentrations (in nucleotides) of DNA with a good signal/noise ratio (Fig. 6 *b*).

Assays based on dsDNA binding dyes can offer good sensitivity, but may result in photocleavage of the DNA substrate or inhibition of the reaction of interest (35,36). Indeed, we were unable to obtain a useful signal for DNA unwinding by the PcrA·RepD system using the dye displacement assay (data not shown). Moreover, the percent loading of the dye on the DNA may affect its binding and fluorescence properties due to crowding of binding sites (37). Finally, there is a fluorescence decrease as ssDNA forms. In contrast, the assay using DCC-SSB exhibits a fluorescence increase on forming ssDNA, making it easier to measure low extents of reaction against a low fluorescence background.

Practical considerations for the use of DCC-SSB in helicase assays revolve in part on the optical properties, as outlined above. Appropriate concentrations of added DCC-SSB will depend on the sensitivity required of the measurement, on the affinity of this protein for DNA, and on a suitable ratio of SSB to DNA. At high ionic strength, the dissociation constant obtained from a titration with dT_{70} is ~2.6 nM. Although this does not take into account potential cooperativity on binding to longer DNA, it gives a guide to the lower limits of concentrations. In addition, to obtain a relatively linear response of ssDNA versus fluorescence, it is important to consider the complexities of the equilibrium binding titrations in different ionic strengths (Fig. 3). A good rule of thumb is to use the equivalent of approximately one monomer of DCC-SSB per five-base length of ssDNA. This should ensure that not only will the DCC-SSB remain in excess over DNA whatever the binding mode, but also the signal response will have approximately a linear response, equivalent to the first part of each titration shown in Fig. 3. Like many fluorescence assays, a calibration curve may be required for complete quantitation. In future work, the probe will provide a tool to understand in detail the kinetics of SSB protein binding to ssDNA as it is progressively produced by a translocating helicase. This situation more closely resembles the physiological functioning of SSB, as opposed to monitoring the direct binding between SSB and naked ssDNA. Moreover, the model ssDNA substrates used here to determine the binding kinetics can only bind one or two SSB molecules, whereas a continuous nucleoprotein filament is (presumably) formed in the helicase measurements. However, preliminary data suggest that the kinetics of binding DCC-SSB to poly(dT) is similar to that described here for dT_{70}.

DCC-SSB can be applied with high temporal resolution and sensitivity to measure helicase activity in bulk solution. Due to the relatively large binding site of SSB protein, this method is well suited to monitor the unwinding of large stretches of dsDNA, rather than the short oligonucleotides employed in many other helicase assays. Therefore, it is of particular use for helicases that are highly processive or can act distributively over an extensive length of DNA. Because of the high sensitivity and increase in fluorescence during dsDNA unwinding, this biosensor or variants based on SSB can potentially be applied to the study of any DNA transaction involving ssDNA intermediates using bulk, high-throughput, or single-molecule techniques.

We thank Dr. J. E. T. Corrie (MRC National Institute for Medical Research, UK) for providing fluorescent labeling reagents, and Joe Yeeles, Dr. Emma Longman, and Dr. Frank Peske (all University of Bristol, UK) for their comments on the manuscript.

This work was supported by the Medical Research Council, UK (K.L.T., J.L.H., M.R.W.), the Wellcome Trust and the Royal Society (M.S.D.), and the National Institutes of Health (R37GM-062653 to S.C.K. and T32GM-007377 to J.C.B.). Part of this work is the subject of a patent application.

REFERENCES

1. Singleton, M. R., M. S. Dillingham, and D. B. Wigley. 2007. Structure and mechanism of helicases and nucleic acid translocases. *Annu. Rev. Biochem.* 76:23–50.
2. Myong, S., M. M. Bruno, A. M. Pyle, and T. Ha. 2007. Spring-loaded mechanism of DNA unwinding by hepatitis C virus NS3 helicase. *Science.* 317:513–516.
3. Martinez-Senac, M. M., and M. R. Webb. 2005. Mechanism of translocation and kinetics of DNA unwinding by the helicase RecG. *Biochemistry.* 44:16967–16976.
4. Lucius, A. L., C. J. Wong, and T. M. Lohman. 2004. Fluorescence stopped-flow studies of single turnover kinetics of *E. coli* RecBCD helicase-catalyzed DNA unwinding. *J. Mol. Biol.* 339:731–750.
5. Roman, L. J., and S. C. Kowalczykowski. 1989. Characterization of the helicase activity of the *Escherichia coli* RecBCD enzyme using a novel helicase assay. *Biochemistry.* 28:2863–2873.
6. Eggleston, A. K., N. A. Rahim, and S. C. Kowalczykowski. 1996. A helicase assay based on the displacement of fluorescent, nucleic acid-binding ligands. *Nucleic Acids Res.* 24:1179–1186.
7. Rye, H. S., M. A. Quesada, K. Peck, R. A. Mathies, and A. N. Giazer. 1991. High-sensitivity two-color detection of double-stranded DNA with a confocal fluorescence gel scanner using ethidium homodimer and thiazole orange. *Nucleic Acids Res.* 19:327–333.
8. Webb, M. R. 2007. Development of fluorescent biosensors for probing the function of motor proteins. *Mol. Biosyst.* 3:249–256.
9. Dwyer, M. A., and H. W. Hellinga. 2004. Periplasmic binding proteins: a versatile superfamily for protein engineering. *Curr. Opin. Struct. Biol.* 14:495–504.
10. Moschou, E. A., L. G. Bachas, S. Daunert, and S. K. Deo. 2006. Hinge-motion binding proteins: unraveling their analytical potential. *Anal. Chem.* 78:6692–6700.
11. Brune, M., J. L. Hunter, S. A. Howell, S. R. Martin, T. L. Hazlett, J. E. T. Corrie, and M. R. Webb. 1998. Mechanism of inorganic phosphate interaction with phosphate binding protein from *Escherichia coli*. *Biochemistry.* 37:10370–10380.
12. Tolosa, L., I. Gryczynski, L. R. Eichhorn, J. D. Dattelbaum, F. N. Castellano, G. Rao, and J. R. Lakowicz. 1999. Glucose sensor for low-cost lifetime-based sensing using a genetically engineered protein. *Anal. Biochem.* 267:114–120.
13. Dattelbaum, J. D., L. L. Looger, D. E. Benson, K. M. Sali, R. B. Thompson, and H. W. Hellinga. 2005. Analysis of allosteric signal transduction mechanisms in an engineered fluorescent maltose biosensor. *Protein Sci.* 14:284–291.
14. Raghunathan, S., A. G. Kozlov, T. M. Lohman, and G. Waksman. 2000. Structure of the DNA binding domain of *E. coli* SSB bound to ssDNA. *Nat. Struct. Biol.* 7:648–652.
15. Raghunathan, S., C. S. Ricard, T. M. Lohman, and G. Waksman. 1997. Crystal structure of the homo-tetrameric DNA binding domain

of *Escherichia coli* single-stranded DNA-binding protein determined by multiwavelength x-ray diffraction on the selenomethionyl protein at 2.9-A resolution. *Proc. Natl. Acad. Sci. USA.* 94:6652–6657.

16. Lohman, T. M., and M. E. Ferrari. 1994. *Escherichia Coli* single-stranded DNA-binding protein: multiple DNA-binding modes and cooperativities. *Annu. Rev. Biochem.* 63:527–570.
17. Kuznetsov, S. V., A. G. Kozlov, T. M. Lohman, and A. Ansari. 2006. Microsecond dynamics of protein-DNA interactions: direct observation of the wrapping/unwrapping kinetics of single-stranded DNA around the *E. coli* SSB tetramer. *J. Mol. Biol.* 359: 55–65.
18. Molineux, I. J., A. Pauli, and M. L. Gefter. 1975. Physical studies of the interaction between the Escherichia coli DNA binding protein and nucleic acids. *Nucleic Acids Res.* 2:1821–1837.
19. Liu, J., N. Qian, and S. W. Morrical. 2006. Dynamics of bacteriophage T4 presynaptic filament assembly from extrinsic fluorescence measurements of Gp32-single-stranded DNA interactions. *J. Biol. Chem.* 281:26308–26319.
20. Yeeles, J. T. P., and M. S. Dillingham. 2007. A dual-nuclease mechanism for DNA break processing by AddAB-type helicase-nucleases. *J. Mol. Biol.* 371:66–78.
21. Singleton, M. R., M. S. Dillingham, M. Gaudier, S. C. Kowalczykowski, and D. B. Wigley. 2004. Crystal structure of RecBCD enzyme reveals a machine for processing DNA breaks. *Nature.* 432:187–193.
22. Zhang, W., M. S. Dillingham, C. D. Thomas, S. Allen, C. J. Roberts, and P. Soultanas. 2007. Directional loading and stimulation of PcrA helicase by the replication initiator protein RepD. *J. Mol. Biol.* 371: 336–348.
23. Corrie, J. E. T. 1994. Thiol-reactive fluorescent probes for protein labelling. *J. Chem. Soc. [Perkin 1]* :2975–2982.
24. Munasinghe, V. R. N., and J. E. T. Corrie. 2006. Optimised synthesis of 6-iodoacetamidotetramethylrhodamine. *ARKIVOC.* (ii):143–149.
25. Lohman, T. M., J. M. Green, and R. S. Beyer. 1986. Large-scale overproduction and rapid purification of the *Escherichia coli* ssb gene product. Expression of the ssb gene under lambda PL control. *Biochemistry.* 25:21–25.
26. Fletcher, A. N., and D. E. Bliss. 1978. Laser dye stability. Part 5. Effect of chemical substituents of bicyclic dyes upon photodegradation parameters. *Appl. Phys.* 16:289–295.
27. Leatherbarrow, R. J. 2001. Grafit Version 5. Erithacus Software Ltd., Horley, UK.
28. Webb, M. R., and J. E. T. Corrie. 2001. Fluorescent coumarin-labeled nucleotides to measure ADP release from actomyosin. *Biophys. J.* 81:1562–1569.
29. Thomas, C. D., D. F. Balson, and W. V. Shaw. 1990. *In vitro* studies of the initiation of Staphylococcal plasmid replication. Specificity of RepD for its origin (*oriD*) and characterization of the RepD-*ori* tyrosyl ester intermediate. *J. Biol. Chem.* 265:5519–5530.
30. Soultanas, P., M. S. Dillingham, F. Papadopoulos, S. E. Phillips, C. D. Thomas, and D. B. Wigley. 1999. Plasmid replication initiator protein RepD increases the processivity of PcrA DNA helicase. *Nucleic Acids Res.* 27:1421–1428.
31. Bianco, P. R., L. R. Brewer, M. Corzett, R. Balhorn, Y. Yeh, S. C. Kowalczykowski, and R. J. Baskin. 2001. Processive translocation and DNA unwinding by individual RecBCD enzyme molecules. *Nature.* 409:374–377.
32. Dillingham, M. S., M. R. Webb, and S. C. Kowalczykowski. 2005. Bipolar DNA translocation contributes to highly processive DNA unwinding by RecBCD enzyme. *J. Biol. Chem.* 280:37069–37077.
33. Chedin, F., and S. C. Kowalczykowski. 2002. A novel family of regulated helicases/nucleases from Gram-positive bacteria: insights into the initiation of DNA recombination. *Mol. Microbiol.* 43:823–834.
34. Kozlov, A. G., and T. M. Lohman. 2002. Stopped-flow studies of the kinetics of single-stranded DNA binding and wrapping around the *Escherichia coli* SSB tetramer. *Biochemistry.* 41:6032–6044.
35. Akerman, B., and E. Tuite. 1996. Single- and double-strand photocleavage of DNA by YO, YOYO and TOTO. *Nucleic Acids Res.* 24:1080–1090.
36. OhUigin, C., D. J. McConnell, J. M. Kelly, and W. J. M. van der Putten. 1987. Methylene blue photosensitised strand cleavage of DNA: effects of dye binding and oxygen. *Nucleic Acids Res.* 15:7411–7427.
37. Carisson, C., M. Johnson, and B. Akerman. 1995. Double bands in DNA gel electrophoresis caused by bis-intercalating dyes. *Nucleic Acids Res.* 23:2413–2420.
38. Brune, M., J. L. Hunter, J. E. T. Corrie, and M. R. Webb. 1994. Direct, real-time measurement of rapid inorganic phosphate release using a novel fluorescent probe and its application to actomyosin subfragment 1 ATPase. *Biochemistry.* 33:8262–8271.